NASA/TM-2004-212671

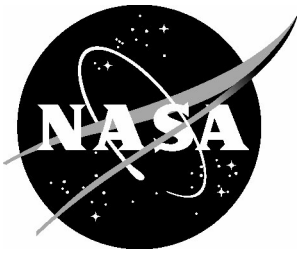

Persistence Characteristics of Wind-Tunnel Pressure Signatures From Two Similar Models

Robert J. Mack
Langley Research Center, Hampton, Virginia

January 2004

The NASA STI Program Office . . . in Profile

Since its founding, NASA has been dedicated to the advancement of aeronautics and space science. The NASA Scientific and Technical Information (STI) Program Office plays a key part in helping NASA maintain this important role.

The NASA STI Program Office is operated by Langley Research Center, the lead center for NASA's scientific and technical information. The NASA STI Program Office provides access to the NASA STI Database, the largest collection of aeronautical and space science STI in the world. The Program Office is also NASA's institutional mechanism for disseminating the results of its research and development activities. These results are published by NASA in the NASA STI Report Series, which includes the following report types:

- TECHNICAL PUBLICATION. Reports of completed research or a major significant phase of research that present the results of NASA programs and include extensive data or theoretical analysis. Includes compilations of significant scientific and technical data and information deemed to be of continuing reference value. NASA counterpart of peer-reviewed formal professional papers, but having less stringent limitations on manuscript length and extent of graphic presentations.

- TECHNICAL MEMORANDUM. Scientific and technical findings that are preliminary or of specialized interest, e.g., quick release reports, working papers, and bibliographies that contain minimal annotation. Does not contain extensive analysis.

- CONTRACTOR REPORT. Scientific and technical findings by NASA-sponsored contractors and grantees.

- CONFERENCE PUBLICATION. Collected papers from scientific and technical conferences, symposia, seminars, or other meetings sponsored or co-sponsored by NASA.

- SPECIAL PUBLICATION. Scientific, technical, or historical information from NASA programs, projects, and missions, often concerned with subjects having substantial public interest.

- TECHNICAL TRANSLATION. English-language translations of foreign scientific and technical material pertinent to NASA's mission.

Specialized services that complement the STI Program Office's diverse offerings include creating custom thesauri, building customized databases, organizing and publishing research results ... even providing videos.

For more information about the NASA STI Program Office, see the following:

- Access the NASA STI Program Home Page at ***http://www.sti.nasa.gov***

- E-mail your question via the Internet to help@sti.nasa.gov

- Fax your question to the NASA STI Help Desk at (301) 621-0134

- Phone the NASA STI Help Desk at (301) 621-0390

- Write to:
  NASA STI Help Desk
  NASA Center for AeroSpace Information
  7121 Standard Drive
  Hanover, MD 21076-1320

NASA/TM-2004-212671

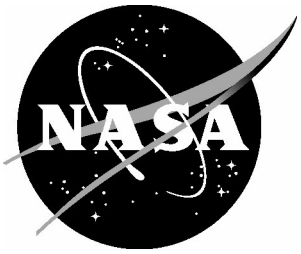

Persistence Characteristics of Wind-Tunnel Pressure Signatures From Two Similar Models

Robert J. Mack
Langley Research Center, Hampton, Virginia

National Aeronautics and
Space Administration

Langley Research Center
Hampton, Virginia 23681-2199

January 2004

Available from:

NASA Center for AeroSpace Information (CASI)
7121 Standard Drive
Hanover, MD 21076-1320
(301) 621-0390

National Technical Information Service (NTIS)
5285 Port Royal Road
Springfield, VA 22161-2171
(703) 605-6000

Summary

Pressure signatures generated by two sonic-boom wind-tunnel models are presented, analyzed, and discussed. The two wind-tunnel models differed in length and span by a factor of about fourteen, but were similar in wing-body planform shape. The geometry of the larger model had been low-boom tailored to generate a "flattop" ground pressure signature, and the nacelles-off pressure signatures from this model at Mach 2 became more "flattop" in shape as the model-probe separation distances increased from 0.94 to 4.4 span lengths. The geometry of the smaller model had not been low-boom tailored, yet its measured pressure signatures had non-N-wave shapes at Mach 2 that persisted as model-probe separation distances increased from 26.0 to 104.2 span lengths. Since the overall planforms of the two wind-tunnel models were so similar, it was concluded that the shape-persistence trends in the pressure signatures of the smaller model would also be present at very large distances in the pressure signatures of the larger model whose geometry had been specifically tailored for low sonic-boom.

Introduction

The practical capabilities of the Whitham Theory, reference 1, the Walkden extension of Whitham Theory to a lifting wing-body, reference 2, and the Seebass and George low-boom minimization theory, reference 3, have been questioned and disputed since the introduction of Computer Fluid Dynamics (CFD) methods to sonic boom analysis. One question concerned the prediction capabilities of the first-order Whitham-Walkden propagation theory. A number of studies (references 4 to 8 are typical) demonstrated the capabilities of Whitham-Walkden theory for predicting the pressure signatures of small wind-tunnel models and high-speed aircraft. Since 1952, the research tools which applied the basic theory, references 9 to 20, were upgraded to improve applicability and prediction accuracy. From a practical application viewpoint, this question could be considered resolved.

A second question concerned the design of wing/fuselage/fin/nacelles concepts with Seebass and George minimization theory; concepts that met both shaped pressure signature and mission range requirements. Results of several NASA Langley studies, references 21 to 26, showed that, with modifications to existing engine-nacelle integration techniques, low-boom minimization methods could be used to successfully design supersonic-cruise conceptual aircraft that had low-boom characteristics. The concepts in these studies ranged in size from 10-passenger business jets to 300-passenger civil transports. So, this question could also be considered resolved.

A third question concerned the persistence of low-boom pressure signature shapes as they passed through the atmosphere from cruise altitude to the ground. Whitham theory could not accurately predict overpressures along the full length of the pressure signatures generated by lifting wing/body models *when these signatures were measured in the near-field of the wind tunnel test section, i.e. model-survey probe distances less than one and possibly as far as ten span lengths*. So, Whitham theory could not be used to extrapolate wind-tunnel-measured pressure signatures from near-cruise altitude to the ground. Thus, the certainty that the model's low-boom tailoring had satisfactorily met the desired ground-level sonic boom requirements could not be completely verified from wind-tunnel data with that theory.

New pressure signature prediction methods, references 27 and 28, were developed from two-dimensional, first-order, cylindrical propagation to extrapolate very-near-field wind-tunnel-measured signatures to the ground. However, these were cylindrical propagation methods, as was Whitham-Walkden theory, so a physical mismatch existed between the three-dimensional character of the measured or CFD-predicted pressure signature flow field, and the theoretical two-dimensional propagation field. Therefore, pressure signature predictions obtained with this methodology could be very inaccurate, and might not completely reflect the merits of low-boom geometry and lift tailoring. Thus, the question of whether these measured pressure signatures would have the desired low-boom shape when they reached the ground remained unanswered.

A preliminary answer to this question of signature shape persistence from cruise altitude to the height of the ground boundary layer was obtained from a 1962 NASA Technical Note, reference 29, and a 1990 NASA Sonic Boom Workshop paper, reference 23. These two reports described, analyzed, and discussed sonic-boom wind-tunnel models, and their measured pressure signatures. Two of the models and their pressure signatures (one model and set of signatures from each referenced report) were selected for analysis and comparisons. Results of this analysis and these comparisons were the basis for judging pressure signature shape persistence. In this paper, these analyses and comparisons of the two selected wind-tunnel models and their measured pressure signatures are presented and discussed.

Nomenclature

b wing span, ft or in

C_L lift coefficient

h cruise altitude, ft; or separation distance, in

I impulse: maximum value of the integral of $\Delta p/p$ along the pressure signature

I_{EXP} impulse calculated from measured pressure signature data (see equation (1))

I_{THEORY} theoretical impulse (see equations (2) and (3))

l overall or effective length, ft or in

L model or non-dimensioning length, ft or in

M Mach number

p free-stream static pressure, psf

Δp incremental free-stream overpressure, psf

S wing area, ft^2

x distance in the longitudinal direction, in

Δx incremental distance in the longitudinal direction, in

Y wind-tunnel separation distance for Model C data, in

β Mach number parameter equal to $(M^2 - 1)^{1/2}$

γ ratio of specific heats equal to 1.4 for air

Low-Boom Methods, Concepts, and Models

Early Sonic-Boom Analysis Methods

Sonic-boom overpressures generated by supersonic-cruise concepts designed during the late twentieth century were estimated with the analysis methods developed between the 1960's when sonic-boom research began in earnest, and the 1980's during the Supersonic-Cruise Air Transport (SCAT) program. These methods were based on equivalent areas, computed from the sum of the volume and lift contributions, to compute an aircraft F-function. Sonic-boom codes used this summed F-function to predict the aircraft's ground pressure signatures. Sources of the volume contributions were the fuselage, the wing, the fin, the canard, and the four engine nacelles. Lift contributions came from the wing, the canard and/or horizontal tail (if they were generating lift at cruise), and the nacelle-wing interference. At that time, all of the aircraft's components were assumed to have equivalent areas that were smooth and continuous. Curved wing leading edges, carefully blended wing-fuselage junctions, and the subsonic leading edges on the wing, canard, and fin(s) were features that readily met the smooth and continuous area-growth criteria. Small nacelle inlet lip angles and negligible interference-lift contributions were also features thought to meet the smoothness criteria.

Sonic-Boom Minimization

The Seebass and George sonic-boom minimization method, reference 3, and its modification by Darden, reference 18, provided practical tools for adding low-boom features to a concept's configuration during the initial stages of preliminary design. A 1990's theory-validation test of these early, and later updated, low-boom analyses and boom minimization methods was made by designing two low-boom aircraft concepts, reference 23. Each concept had a different design Mach number, and generated a different low-boom pressure signature shape. One of these low-boom concepts is discussed in this report, the one that generated a "flat top" ground pressure signature at a Mach number of 2.0. In the following sections, this Mach 2 low-boom concept and model are described, the pressure signature data produced from the model are analyzed, and the significant characteristics of these pressure signatures are interpreted.

Mach 2 Concept and Model

The Mach 2 concept was designed with the low-boom method of reference 3. Its wing planform, derived from a configuration described in reference 22, had a sharply-rounded apex that blended into a long, highly-swept strake. Behind the strake, wing leading edges had sweep angles that changed smoothly from root to tip. Wing dihedral was added to keep the effective and the total lifting length about the same at cruise angle of attack. The center-line camber of the fuselage was contoured to blend into and out of the camber line of the wing root chord to promote smooth wing-fuselage integration.

This Mach 2 concept differed from previous low-boom research concepts in three ways. First, the wing was given a mild camber and twist distribution. Second, it had four engine nacelles hung on short struts under the wing, and third, it had a vertical fin on the aft fuselage. Each of the engine nacelles on the Mach 2 concept was simulated by a ducted body of revolution. A three view schematic of the Mach 2 theory-validation concept is shown in figure 1.

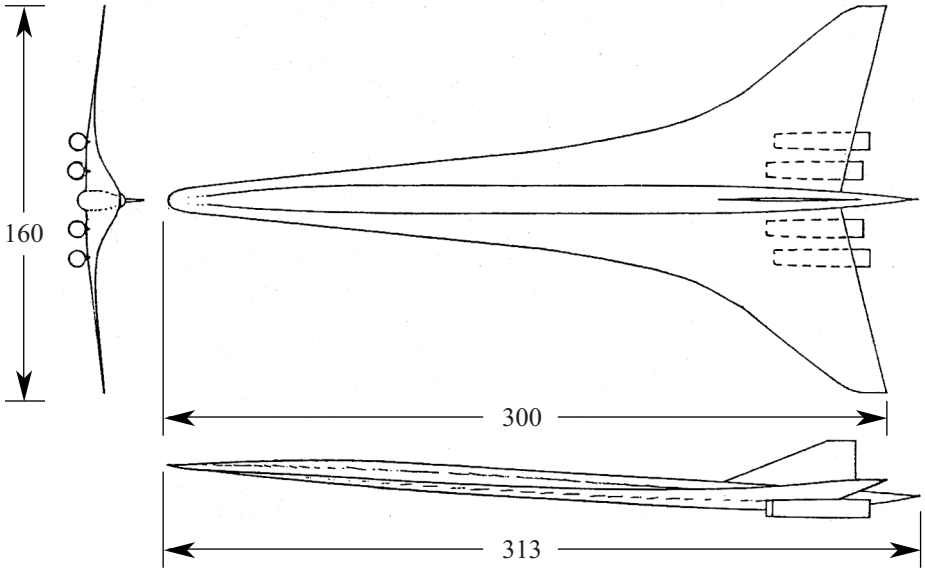

Figure 1. Three view of the Mach 2 theory-validation concept. Lengths are in feet.

Dimensions and low-boom design data for the Mach 2 concept are listed in Appendix A.

A wind-tunnel model of the Mach 2 concept was built. At 1:600 scale, it was 12 inches long, and supported by an integral sting/balance that extended from the aft fuselage. All four nacelles, made from stainless-steel tubing, had constant-area ducts and sharp inlet lips.

Mach 2 Model Pressure Signhatures

Pressure signatures generated by the Mach 2 model, with nacelles on and nacelles off, were measured at separations distances of 6, 12, and 28 inches. A measured pressure signature from the Mach 2 model with nacelles on at a cruise $C_L = 0.068$ is shown in figure 2.

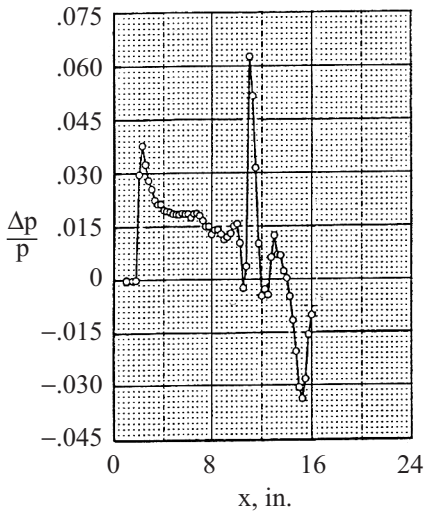

Figure 2. Mach 2 model pressure signature. Sharp-lip metal nacelles, M = 2, h = 6 inches, $C_L = 0.068$.

Nose, tail, and intermediate shocks appeared over finite distances instead of being abrupt due to model vibration, finite orifice size, probe boundary layer, and wind-tunnel turbulence. These effects were identified, analyzed, and discussed in reference 4.

The unexpected pressure rise between the nose shock and the expansion to the tail shock seemed to be due to the nacelles. This idea was tested by measuring another pressure signature at the same distance with the nacelles off. This second signature is seen in figure 3.

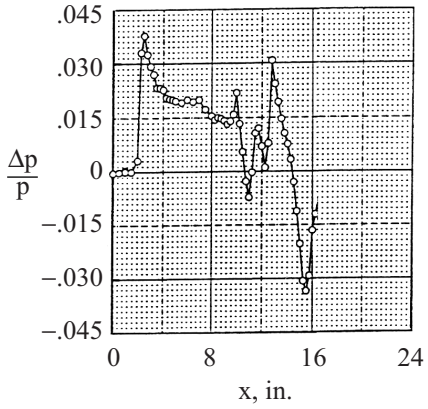

Figure 3. Mach 2 model pressure signature. Nacelles off, M = 2, h = 6 inches, C_L = 0.068.

Several small shocks are seen aft of the nose shock and ahead of the expansion preceding the tail shock, but the large shock has disappeared. So, the pressure signatures in figures 2 and 3 demonstrated that low-boom characteristics of a vehicle could be severely compromised if it had under-the-wing nacelles. Alternative low-boom locations for the nacelles are described in references 20, 24, and 25, along with methods useful for predicting these locations.

Attenuation effects on the nacelles-off Mach 2 model pressure signature were studied on a signature measured at a distance of 12 inches. This signature is shown in figure 4.

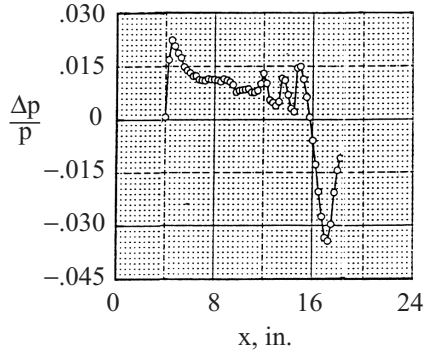

Figure 4. Mach 2 model pressure signature. Nacelles off, M = 2, h = 12 inches, C_L = 0.068.

The pressure disturbances behind the nose shock and ahead of the expansion to the tail shock, have noticeably decreased in strength as expected. However, they have not moved forward as the separation distance increased. They lost more strength through attenuation than did the nose shock, and the mean overpressure level had decreased from the level observed on the pressure signature shown in figure 3. So, the positive overpressure points in figures 2 to 4, ignoring for a

moment the prominent nacelle shock in figure 2, showed a trend toward becoming more "flat top" with increased separation distance.

The nacelles-off pressure signature features and trends, noted in figure 3 and 4, were also observed on a pressure signatures measured at a separation distance of about 28 inches. Figure 5 shows this nacelles-off pressure signature generated at a $C_L = 0.072$, which though about 5.9 percent higher, was closest to the design C_L value.

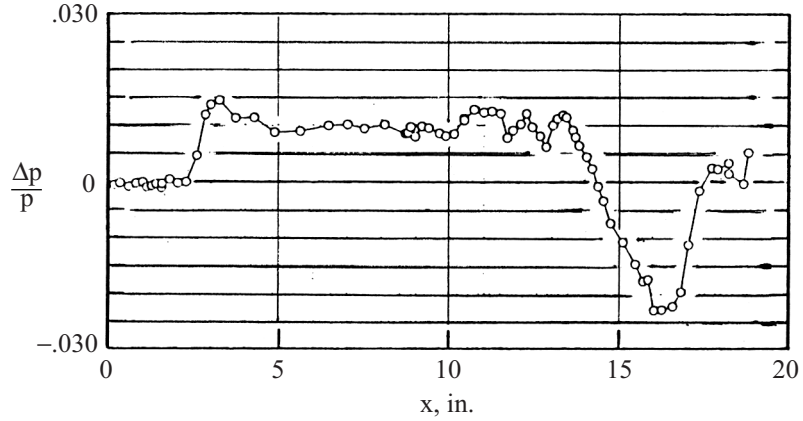

Figure 5. Mach 2 model pressure signature[1]. Nacelles off, M = 2, h = 28 inches, $C_L = 0.072$.

In figure 5, the measured pressure signature was rapidly acquiring a "flat-top" shape at a model/probe separation distance of 28 inches, i.e. a separation distance to span ratio, *h/b*, of 4.375. This was occurring even though the model was at $C_L = 0.072$ which was almost 6 percent higher than the design value. Ignoring the nose shocks in the last three figures, and the nacelle shock observed in figure 2, the incremental disturbances along the top of the pressure signatures in figures 2 to 5 showed a continuous and rapid decrease in strength. At the same time, there was no indication of them moving forward toward coalescence with the nose shock as the separation distance increased, which strongly suggested that they would continue to be discrete and unique as they lost strength with increasing distance. At a large, but not a far-field, distance, these disturbances would disappear and the pressure signature would be completely "flat-top" in shape. This was the desired signature shape obtained from the low-boom minimization code for a vehicle with a Mach 2 concept's and wind-tunnel model's low-boom geometry.

A vehicle cruising at an altitude of 60,000 feet with a wing span of 150 feet would be 400 span lengths above the ground. Obviously, pressure signatures at a height of 400 span lengths could not be measured in a wind tunnel with the Mach 2 model. However, there were measured pressure signatures obtained at *h/b* ratios that more closely approached cruise-field/far-field conditions. These pressure signatures, and the model that generated them, are presented, analyzed, and discussed in the next section.

[1] Data courtesy of Joel Mendoza and Raymond Hicks of the NASA Ames Research Center.

Model C

Three models were used in the wind-tunnel study to determine the influence of wing position on sonic-boom flow-field disturbances, reference 29. The model of interest, Model C, was the third of the three delta-wing/body wind-tunnel model group used in the study. Plan and side views of this model are shown in figure 6.

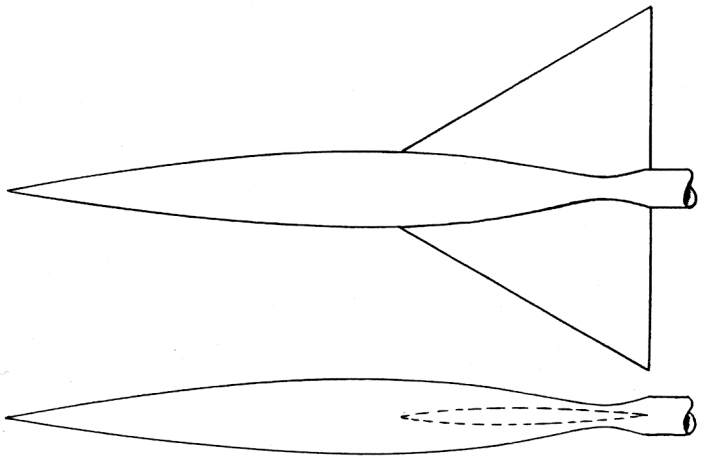

Figure 6. Planform and side view of wind-tunnel Model C.

The forebody was a parabolic body-of-revolution which blended into a "coke-bottled" fuselage. A flat camber surface delta wing straddled the aft "coke-bottled" section of the body. Dimensions of this wind-tunnel model are listed in Appendix B.

Model C was sized to measure pressure signatures at almost far-field distances in a 4- by 4-foot wind tunnel test section. For comparison purposes, its geometry was scaled up to the Mach 2 model size. Results of this comparison are presented in figure 7.

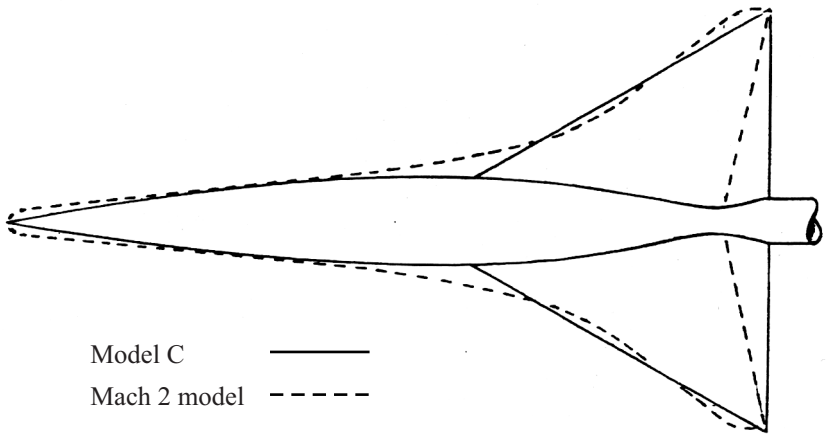

Figure 7. Comparison of the Mach 2 and the Model C fuselage-wing planforms.

The overlaid outlines, in figure 7, show that the two wing-fuselage planforms were remarkably similar even though the methods used to design them were not. The Mach 2 concept and its wind-tunnel model were designed with the low-boom methods of reference 3. It was an all-wing configuration with a mild camber and twist in its low-thickness surfaces. The forward section had a blunted apex that started the lift quickly but with a low lift gradient, and a highly-swept strake behind it to control the growth of that lift. Aft of the strake, the leading-edge sweep gradually decreased so that the lift would grow more rapidly and reach its peak at the wing-tip trailing edge.

Model C, on the other hand, was a simpler configuration having only a flat delta wing and a fuselage. The fuselage forebody was the forward half of a parabolic body of revolution, while the "wasp-waisted" aft body covered the flat-camber-surfaced delta wing. This forebody developed a small amount of slender-body lift which reached its peak by the time the wing lift began to grow and affect the flow field. The wing continued the lift growth from the forebody, and reached its maximum at the wing tip trailing edge. Although designed neither for low boom, nor with low-boom methods, the Model C configuration generated pressure signatures that were very similar in persistence characteristics, though not identical, to those of the low-boom Mach 2 model which was about 14 times larger in length and span. This will be seen in the following sections.

Model C Pressure Signatures

Pressure signatures generated by Model C were measured at three lift conditions and three separation distances. The lift on the model corresponded to lift coefficients of $C_L = 0.0$, 0.10, and 0.20 while the model-probe separation distances corresponded to distance/span ratios, h/*b*, of 26.0, 52.1, and 104.2.

With $C_L = 0.0$, only volume effects from the fuselage and the wing were present in the pressure signatures. At $C_L = 0.10$ (a lift coefficient typical of supersonic-cruise configurations at beginning-cruise altitude and weight) the flow-field disturbances were generated by both fuselage and wing volume and wing lift effects. At a $C_L = 0.20$, the lift contribution was so much larger than that of the volume, that it completely overshadowed the foreshortened fuselage and wing volume effect. As a result, the pressure signature was an N-wave at all wind-tunnel test section separation distances. Moreover, at a $C_L = 0.20$, the model was much farther from the design C_L and the design lift/drag ratio of the Mach 2 concept and wind-tunnel model than at a $C_L = 0.10$. So, only the pressure signatures measured at the three wind-tunnel-study separation distances and at $C_L = 0.0$ and 0.10 are presented for comparison purposes. Of these pressure signatures, only the signatures measured at $C_L = 0.10$ are used in the theoretical comparisons. These six Model C wind-tunnel pressure signatures are presented in figures 8 through 10.

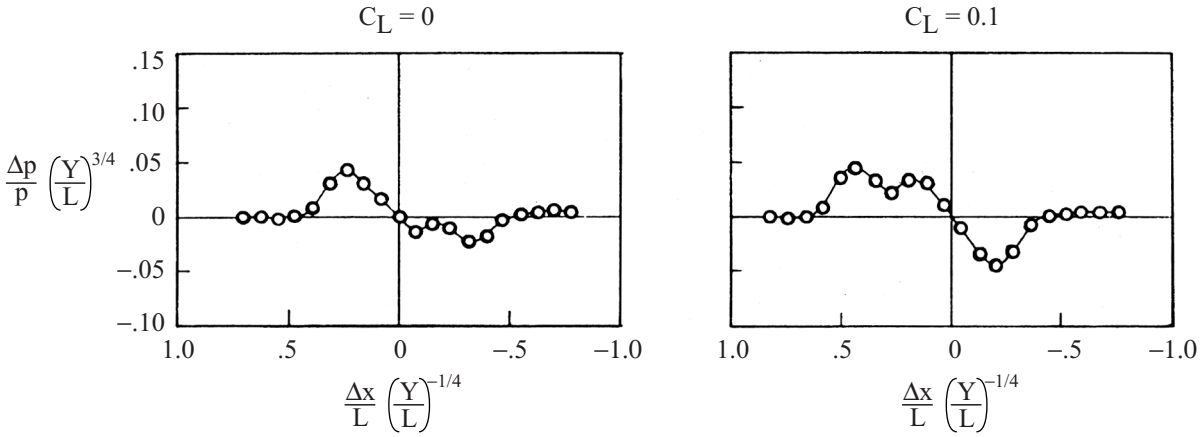

Figure 8. Model C pressure signatures at M = 2.01, *h/b* = 26.0, C_L = 0.0 and 0.10.

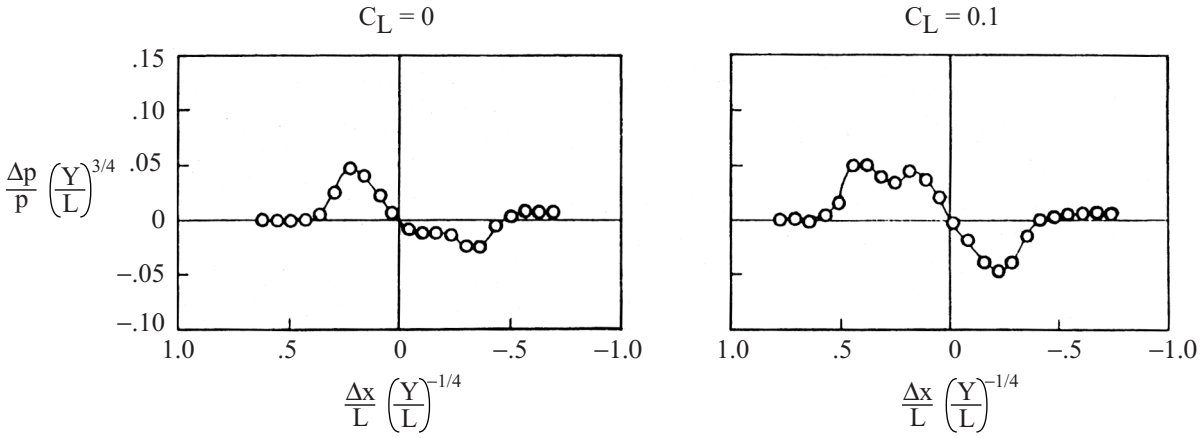

Figure 9. Model C pressure signatures at M = 2.01, *h/b* = 52.1, C_L = 0.0 and 0.10.

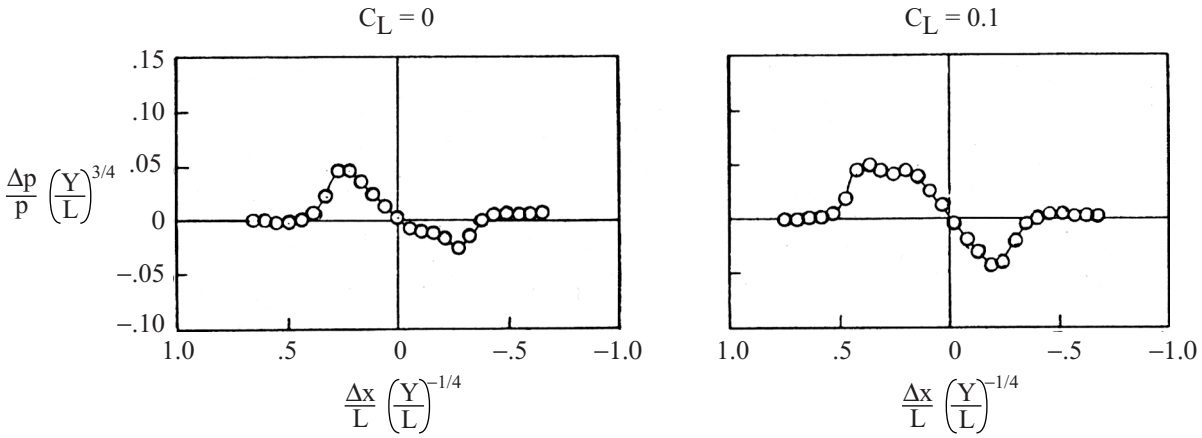

Figure 10. Model C pressure signature at M = 2.01, *h/b* = 104.2, C_L = 0.0 and 0.10.

The pressure signatures in figures 8 to 10 were plotted in far-field pressure-ratio and distance-ratio parameters. In this parametric format, trends in the shapes of the pressure signatures to

become “N-wave” shapes could be easily seen, and in the far-field, “N-wave” pressure signatures would be identical at all large separation distances.

On the Model C pressure signatures, as on the Mach 2 model pressure signatures, all the measured shocks were rounded instead of being abrupt jumps due to model vibration, finite orifice size, and probe boundary layer. These effects were discussed in reference 4.

Disturbances from the model nose were due mostly to volume effects. These effects produced a nose shock with about the same strength in the first signature peak at $C_L = 0.0$ as at $C_L = 0.10$. The wing lift effects appeared mainly as the second peak on pressure signatures at the three separation distances when $C_L = 0.10$, even though a small amount of lift was generated by the circular cross section forebody. At both $C_L = 0.0$ and 0.10, these pressure signatures were interesting because their near-field shape characteristics (none of them had a far-field N-wave shape) extend from distance ratios of $h/b = 26.0$ to $h/b = 104.2$. This unforeseen but fortuitous characteristic was noted in the reference 29 report of a study done almost ten years before the introduction of the Seebass and George minimization theory of reference 3.

Another way to determine the trend toward far-field characteristics for pressure signatures is to plot “impulse” versus separation distance or separation/span ratio. Measured, or experimental, pressure signature “impulse” can be defined as:

$$I_{EXP} = \text{Measured Impulse} = \int \frac{\Delta p}{p} d\left(\frac{x}{l}\right)\Bigg|_{maximum} \tag{1}$$

The theoretical value of the impulse is expressed as:

$$I_{THEORY} = \text{Theoretical Impulse} = \gamma \frac{M^2}{\sqrt{2\beta}} \sqrt{\frac{l}{h}} \int \frac{F(y)}{\sqrt{l}} d\left(\frac{y}{l}\right)\Bigg|_{maximum} \tag{2}$$

and is calculated from the concept’s or model’s volume and lift distributions. It can be seen from equation (2) that

$$I_{THEORY} \sqrt{\frac{h}{l}} = \frac{\gamma M^2}{\sqrt{2\beta}} \int \frac{F(y)}{\sqrt{l}} d\left(\frac{y}{l}\right)\Bigg|_{maximum} = \text{constant} \tag{3}$$

which, in some ways, is a more convenient form of equation (2). This equation is useful for comparisons of the impulse derived from measured and predicted pressure signatures, or from measured pressure signatures and the model’s or concept’s F-function.

When the measured impulse values of the Model C pressure signatures at $C_L = 0.10$ were compared with the theoretical values for a $C_L = 0.10$, a poor agreement was found. Changing the lift coefficient from $C_L = 0.10$ to $C_L = 0.133$ and recalculating the F-function of the model with the new lift distribution brought the measured and predicted values into closer agreement. This comparison of measured and theoretical impulse values was done with equation (3) for the two values of the lift coefficient, and is shown in figure 11.

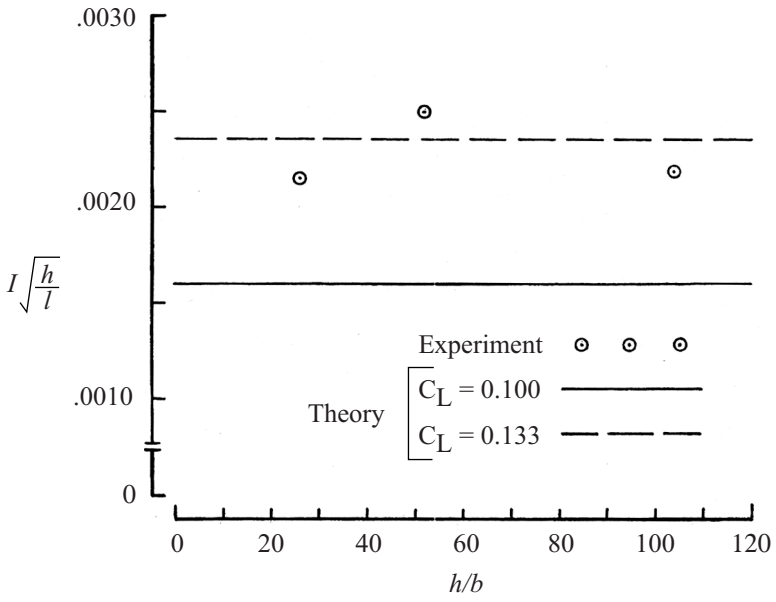

Figure 11. Comparison of measured and theoretical values of impulse with C_L = 0.10 and 0.133.

These results strongly suggested that Model C pressure signatures were really measured at C_L = 0.133 rather than at C_L = 0.10. So, the pressure signature in figure 10, measured at *h/b* = 104.2 and a C_L value of 0.10, was compared with pressure signatures predicted with Whitham Theory methods at *h/b* = 104.2 and C_L values of 0.10 and 0.133. This comparison is shown in figure 12.

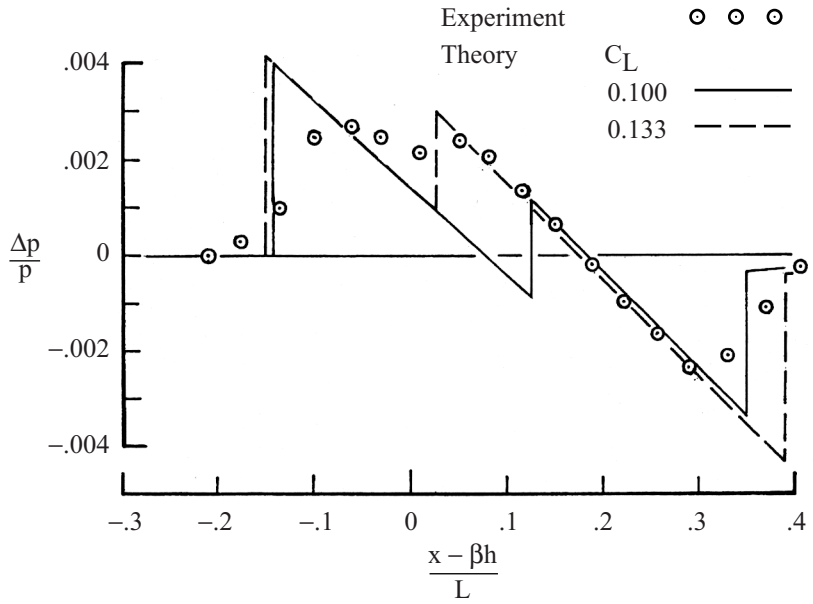

Figure 12. Measured and predicted Model C pressure signatures. M = 2.01 and *h/b* = 104.2. Signatures were predicted at C_L = 0.10 and 0.133, L = 4.0 inches.

A much better agreement between the measured and the predicted pressure signatures was achieved with the model at a $C_L = 0.133$ rather than at $C_L = 0.10$, the text value of reference 29. This result was in agreement with the conclusion reached after the comparison of measured and theoretical values of pressure signature impulse shown in figure 11. A $C_L = 0.10$ would be obtained with the model at an angle of attack of 2.64 degrees, while a value of $C_L = 0.133$ would be obtained at 3.50 degrees. The difference in C_L values was attributed to the difficulty in accurately setting the angle of attack of the small model by hands-on bending of the sting, and to small flexures along the sting when the model was at lift conditions (see reference 22).

Increasing the lift on a model or a concept usually enhances tendencies for a low-boom-shaped pressure signature, or a pressure signature with near-field features, to change abruptly to an N-wave pressure signature. This shape instability, i.e. likelihood for an abrupt change from a low-boom shaped (or a quasi-low-boom shaped) to an N-wave pressure signature, was not observed in the Model C measured or predicted pressure signatures. So, it was concluded from an analysis of data in figures 8 to 10 and 12, that pressure signatures generated by Model C would not degenerate into N-waves until separation distance/span ratios much greater than 104.2 were reached. The most probable reason for this fortuitous circumstance was that the volume and lift distribution in the Model C geometry was very close to, but not exactly the same as, a low-boom equivalent area distribution.

Results

Although the geometry of Model C had not been designed with low-boom minimization methods, nor had its geometry been tailored to generate low-boom pressure signatures, the pressure signature data suggested that such designing and tailoring had fortuitously been done. The pressure signatures generated at a $C_L = 0.10$ showed noticeable shape-persistence characteristics, i.e. the shape of the pressure signature at $h/b = 26.0$ looked very much like the pressure signature at $h/b = 104.2$ when both pressure signatures were plotted in far-field parametric form. Although the "hint" of a small shock was observed between the nose shock and the expansion to the tail shock, the pressure signature measured at the farthest model-survey probe separation distance, $h/b = 104.2$, had a positive-pressure top that appeared to have tendencies toward becoming almost "flat topped" in appearance.

The Mach 2 wind-tunnel model, without nacelles, had pressure signatures with several small shocks along the positive-pressure part of the signature. As the separation distance increased from 6.0 to 28.0 inches, these small shocks gradually dissipated without moving forward to coalesce with the nose shock, leaving the positive part virtually "flat topped" in shape. This asymptotic trend toward becoming and remaining flat-topped was very similar to the trend toward retaining non-N-wave characteristics seen on Model C pressure signatures measured at $h/b = 26.0$ to 104.2. Pressure signature shape "freezing" was predicted to occur on the Mach 2 Concept ground pressure signature under the flight path at start of cruise, and the wind-tunnel data from these two models strongly suggested that these effects might be realized in real atmosphere propagation.

Concluding Remarks

The Mach 2 wind-tunnel model, with nacelles off, and the Model C wind-tunnel model were simple wing-fuselage configurations with very similar planform shapes. Measured pressure signatures from both models had identifiable signature persistence trends with increasing separation distance below the flight path. The Model C wind-tunnel data at h/b = 26.0, 52.1, and 104.2, and the results of the model's sonic-boom analysis lead to the conclusion that the pressure signature shape of Model C would persist from cruise altitude to the ground if Model C were to be scaled up to a full-sized supersonic-cruise concept. Since the Model C planform and configuration geometry had shown strong pressure signature persistence characteristics, and the geometry of the Mach 2 model (and concept) was so similar, it was concluded that the pressure signature shapes of the Mach 2 concept and model would also retain their low-boom characteristics from h/b = 4.375 to h$/b$ = 104.2*, and then to the ground.* Thus, it was concluded that these observations could be generalized to predict a low-boom signature generated by a suitably-tailored wing-fuselage configuration would persist from cruise altitude to the ground once it had been established in the atmosphere above 36,000 feet.

The analysis in this paper, as well as the report that described and discussed the Model C wind-tunnel data, demonstrated that small wind-tunnel models could still be useful in sonic boom research. However, the goals of the experiment that employed such small models had to be limited in scope, e.g. the determination of shape evolution, attenuation, and persistence, the effect of wing planform on pressure signature shape, or the effects of engine nacelles and/or nacelle shapes on the flow field.

Although the results of this study demonstrated that the wind-tunnel model's small size was not a serious detriment to obtaining meaningful sonic-boom data in the wind tunnel, they could not be construed as a blanket endorsement of very small models or as an endorsement for the use of small models for out-of-plane-of-symmetry measurements of overpressures. There will always be a need for increased model size when the effects of the vehicle's components, such as the engine nacelles, on the flow-field of a complete configuration must be studied. As long as the goals of the test are limited to simple identifiable characteristics, then the possibility of using models in the range of three to five inches in length should be considered.

It should be noted, however, that these test results indicate only that, with properly-configured small models, low-boom pressure signature shapes will show persistence characteristics in wind-tunnel test sections and in non-turbulent, calm, standard atmospheres. *They do not and cannot predict shape persistence for pressure signatures that pass through an atmosphere* filled with turbulence, wind shear, and temperature gradients; common features usually found in the layer of air 3000 to 5000 feet above the ground. The characteristics of this "last mile" of atmosphere were studied over forty years ago with the intention of simulating them in the wind tunnel. No practical method for fully achieving this simulation was ever found, so including these effects are outside the scope of this paper. These areas of unresolved and unanswered questions resurrected and reinforced the conclusion that the measurements of these real atmospheric effects would probably have to be made with a full-scale low-boom-configured aircraft making a large number of flights over extensive microphone arrays, or having an instrumented aircraft make multiple passes back and forth through the flow field around such a research aircraft.

References

1. Whitham, G. B.: *The Flow Pattern of a Supersonic Projectile*. Communications on Pure and Applied Mathematics vol. V, no. 3, August 1952, pp. 301-348.

2. Walkden, F.: *The Shock Pattern of a Wing-Body Combination, Far From the Flight Path*. Aeronautical Quarterly, vol. IX, pt. 2, May 1958, pp. 164-194.

3. Seebass, R.; and George, A. R.: *Sonic-Boom Minimization.* Journal of the Acoustical Society of America, vol. 51, no. 2, pt. 3, February 1972, pp. 686 - 694.

4. Carlson, Harry W.: *Correlation Of Sonic-Boom Theory With Wind-Tunnel And Flight Measurements*, NASA TR R-213, December 1964.

5. Carlson, Harry W.; Mack, Robert J.; and Morris, Odell A.: *Sonic-Boom Pressure Field Estimation Techniques*. Proceedings of the Sonic Boom Symposium, November 3, 1965.

6. Kane, E. J.: *Some Effects Of The Nonuniform Atmosphere On The propagation Of Sonic Booms*, Proceedings of the Sonic Boom Symposium, November 3, 1965.

7. Carlson, H. W.; and Maglieri, D. J.: *Review Of Sonic-Boom Generation And Prediction Methods.* Proceedings of the Second Sonic Boom Symposium, November 3, 1970.

8. Hayes, Wallace D.; and Runyan, Harry L.: *Sonic-Boom Propagation Through A Stratified Atmosphere.* Proceedings of the Second Sonic Boom Symposium, November 3, 1970.

9. Middleton, Wilbur D.; and Carlson, Harry W.: *A Numerical Method For Calculating Near-Field Sonic-Boom Pressure Signatures.* NASA TN D-3082, 1965.

10. McLean, F. Edward; and Shrout, Barrett L.: *Design Methods For Minimization Of Sonic-Boom Pressure-Field Disturbances*. Proceedings of the Sonic Boom Symposium, November 3, 1965.

11. Kane, E. J.: *Some Effects Of The Nonuniform Atmosphere On The propagation Of Sonic Booms*, Proceedings of the Sonic Boom Symposium, November 3, 1965.

12. Harris, Roy V., Jr.: *A Numerical Technique for Analysis of Wave Drag at Lifting Conditions*. NASA TN D-3586, 1966.

13. Mack, Robert J.: *A Numerical Method for Evaluation and Utilization of Supersonic Nacelle-Wing Interference*. NASA TN D-5057, 1969.

14. Hayes, Wallace D.; Haefeli, Rudolph C.; and Kulsrud, H. E.: *Sonic Boom Propagation In A Stratified Atmosphere, With Computer Program*. NASA CR-1299, 1969.

15. Craidon, Charlotte B.: *Description Of A Digital Computer Program For Airplane Configuration Plots*. NASA TM X-2074, 1970.

16. Carlson, Harry W.; and Mack, Robert J.: *Estimation Of Attainable Leading-Edge Thrust For Supersonic Wings Of Arbitrary Planform*. NASA TP 1270, October 1978.

17. Carlson, Harry W.; and Mack, Robert J.: *Estimation Of Leading-Edge Thrust For Wings At Subsonic And Supersonic Speeds*. NASA TP 1500, October 1979.

18. Darden, Christine M.: *Sonic Boom Minimization With Nose-Bluntness Relaxation.* NASA TP-1348, 1979.

19. Carlson, Harry W.; and Mack, Robert J.: *Estimation Of Wing Nonlinear Aerodynamic Characteristics at Supersonic Speeds*. NASA TP-1718, 1980.

20. Mack, Robert J.: *Some Considerations on the Integration of Engine Nacelles into Low-Boom Aircraft Concepts*. High-Speed Research: Sonic Boom, Volume II, NASA Conference Publication 3173, 1992.

21. Carlson, Harry W.; Barger, Raymond L.; and Mack, Robert J.: *Application Of Sonic-Boom Minimization Concepts In Supersonic Transport Design*. NASA TN D-7218, June 1973.

22. Mack, Robert J.; and Darden, Christine M.: *Wind-Tunnel Investigation Of The Validity Of A Sonic-Boom-Minimization Concept.* NASA TP 1421, October 1979.

23. Mack, Robert J.; and Needleman, Kathy E.: *The Design Of Two Sonic Boom Wind Tunnel Models From Conceptual Aircraft Which Cruise At Mach Numbers Of 2.0 And 3.0*. AIAA-90-4026, AIAA 13th Aeroacoustics Conference, October 22-24, 1990.

24. Mack, Robert J.: *Low-Boom Aircraft Concept With Aft-Fuselage-Mounted Engine Nacelles*. High-Speed Research: Sonic Boom, Volume II, NASA CP-10133, February 1994.

25. Mack, Robert J.: *A Supersonic Business-Jet Concept Designed For Low Sonic Boom*. NASA/TM-2003-212435, October 2003.

26. Mack, Robert J.: *An Analysis Of Measured Sonic-Boom Pressure Signatures From A Langley Wind-Tunnel Model Of A Supersonic-Cruise Business Jet Concept.* NASA/TM-2003-212447, October 2003.

27. Hicks, Raymond M.; and Mendoza, Joel P.: *Prediction of Sonic Boom Characteristics From Experimental Near Field Results*. NASA TM X-1477, September 1967.

28. Thomas, Charles L.: *Extrapolation Of Wind-Tunnel Sonic Boom Signatures Without Use Of A Whitham F-function*. Third Conference on Sonic Boom Research, NASA SP-255, 1971.

29. Morris, Odell A.: *A Wind-Tunnel Investigation At A Mach Number Of 2.01 Of The Sonic-Boom Characteristics Of Three Wing-Body Combinations Differing In Wing Longitudinal Location.* NASA TN D-1384, September 1962.

Appendix A

Mach 2 Low-Boom Concept Design Data

The Mach 2 concept was designed to validate low-boom analysis and design methodology that had been developed prior to the close of the supersonic-cruise aircraft research programs. It was designed to generate ground-level overpressures of about 1.0 psf while cruising at its design Mach number and cruise altitude. No attempts were made to size the concepts for enhanced mission performance or minimum weight. The beginning-cruise weight, used to calculate sonic boom, was estimated from previous high-technology concepts. Wing planform shapes, areas, spans, and dihedrals were selected primarily to match the concept's equivalent area distribution to a Seebass and George low-boom equivalent area distribution. Features that reduced both sonic boom and aerodynamic drag were kept; those that increased sonic-boom overpressures were bypassed even though they may have reduced aerodynamic drag or empty weight. Therefore, no gross take-off weights, empty weights, fuel weights, etc. are listed in the data below, because they are the results of sizing and shaping the configuration for minimum weight and maximum mission performance.

	Mach 2 Concept
Span, b , ft	160.0
Length, l , ft	313.0
Wing Lift Length, ft	300.0
Wing Area, S, ft^2	15,055.0
Aspect Ratio, b^2/S	1.70
Beginning Cruise Altitude, h , ft	55,000.0
Beginning Cruise Weight, lb	550,000.0
Cruise Mach Number, M	2.0
Cruise C_L	0.06803
Number Of Engines	4
Ground-Level Shock Overpressure, psf	1.0
Type Of Low-Boom Signature Shape, reference 3	"Flat-Top"

Appendix B

Model C Design Data and Dimensions

The Model C wind-tunnel model was one of three wing-body models used to determine the effects of wing position on the sonic-boom overpressures of a wing-body configuration in supersonic-cruise flight, reference 29. Basic wing and fuselage shapes were the same for all three models, but the wings were placed in three locations. On Model A, the wind apex was almost, but not quite, coincident with the fuselage nose. For Model B, the wing was positioned aft of the nose, about half way along the overall length of the fuselage. On Model C, the model described in this report along with a sample of its pressure signatures, the wing trailing edge was coincident with the aft end of the wind-tunnel model and with the front edge of the model sting.

	Model C
Span, b , ft	0.48
Overall Length, l, in	1.00
Wind-Tunnel Model Length, L , in	0.85
Wing Area, S, in^2	0.09977
Aspect Ratio, b^2/S	2.3
Circular Airfoil Thickness Ratio	0.048
Test Mach Number, M	2.01
Leading-Edge Sweep Angle, deg	60.0
Test C_L values	0.0, 0.10, 0.20

REPORT DOCUMENTATION PAGE

Form Approved
OMB No. 0704-0188

1. REPORT DATE *(DD-MM-YYYY)*	2. REPORT TYPE	3. DATES COVERED *(From - To)*
01- 01 - 2004	Technical Memorandum	

4. TITLE AND SUBTITLE
Persistence Characteristics of Wind-Tunnel Pressure Signatures From Two Similar Models

5a. CONTRACT NUMBER

5b. GRANT NUMBER

5c. PROGRAM ELEMENT NUMBER

6. AUTHOR(S)
Mack, Robert J.

5d. PROJECT NUMBER

5e. TASK NUMBER

5f. WORK UNIT NUMBER
23-706-92-02

7. PERFORMING ORGANIZATION NAME(S) AND ADDRESS(ES)
NASA Langley Research Center
Hampton, VA 23681-2199

8. PERFORMING ORGANIZATION REPORT NUMBER
L-18340

9. SPONSORING/MONITORING AGENCY NAME(S) AND ADDRESS(ES)
National Aeronautics and Space Administration
Washington, DC 20546-0001

10. SPONSOR/MONITOR'S ACRONYM(S)
NASA

11. SPONSOR/MONITOR'S REPORT NUMBER(S)
NASA/TM-2004-212671

12. DISTRIBUTION/AVAILABILITY STATEMENT
Unclassified - Unlimited
Subject Category 05
Availability: NASA CASI (301) 621-0390 Distribution: Standard

13. SUPPLEMENTARY NOTES
An electronic version can be found at http://techreports.larc.nasa.gov/ltrs/ or http://ntrs.nasa.gov

14. ABSTRACT

Pressure signatures generated by two sonic-boom wind-tunnel models and measured at Mach 2 are presented, analyzed, and discussed. The two wind-tunnel models differed in length and span by a factor of fourteen, but were similar in wing-body planform shape. The geometry of the larger model had been low-boom tailored to generate a "flat top" ground pressure signature, and the nacelles-off pressure signatures from this model became more "flattop" in shape as the model-probe separation distances increased from 0.94 to 4.4 span lengths. The geometry of the smaller model had not been low-boom tailored, yet its measured pressure signatures had non-N-wave shapes that persisted as model-probe separation distances increased from 26.0 to 104.2 span lengths. Since the overall planforms of the two wind-tunnel models were so similar, it was concluded that the shape-persistence trends in the pressure signatures of the smaller, non-low-boom tailored model would also be present at very large distances in the pressure signatures of the larger, low-boom-tailored model.

15. SUBJECT TERMS
Sonic boom; Wind-tunnel models; Pressure signature persistence; Low-boom characteristics

16. SECURITY CLASSIFICATION OF:			17. LIMITATION OF ABSTRACT	18. NUMBER OF PAGES	19a. NAME OF RESPONSIBLE PERSON
a. REPORT	b. ABSTRACT	c. THIS PAGE			STI Help Desk (email: help@sti.nasa.gov)
					19b. TELEPHONE NUMBER *(Include area code)*
U	U	U	UU	23	(301) 621-0390